Published in final edited form as:
*Dev Biol*. 2008 January 1; 313(1): 384–397. doi:10.1016/j.ydbio.2007.10.029.

# Overexpression of PPK-1, the *C. elegans* Type 1 PIP kinase, inhibits growth cone collapse in the developing nervous system and causes axonal degeneration in adults

**David Weinkove**[2,3,*], **Michael Bastiani**[1,*], **Tamara A. M. Chessa**[2,†], **Deepa Joshi**[1], **Linda Hauth**[1], **Frank T. Cooke**[4], **Nullin Divecha**[2,§], and **Kim Schuske**[1]

[1] Department of Biology, University of Utah, Salt Lake City UT 84112-0840

[2] Division of Cellular Biochemistry, Netherlands Cancer Institute, 1066 CX Amsterdam

[3] Department of Biology, University College London, Gower Street, London WC1E 6BT, UK

[4] Department of Biochemistry and Molecular Biology, University College London, Gower Street, London WC1E 6BT, UK

## Abstract

Growth cones are dynamic membrane structures that migrate to target tissue by rearranging their cytoskeleton in response to environmental cues. The lipid phosphatidylinositol (4,5) bisphosphate ($PIP_2$) resides on the plasma membrane of all eukaryotic cells and is thought to be required for actin cytoskeleton rearrangements. Thus $PIP_2$ is likely to play a role during neuron development, but this has never been tested *in-vivo*. In this study we have characterized the $PIP_2$ synthesizing enzyme Type 1 PIP kinase (*ppk-1*) in *Caenorhabditis elegans*. PPK-1 is strongly expressed in the nervous system, and can localize to the plasma membrane. We show that PPK-1 purified from *C. elegans* can generate $PIP_2$ *in-vitro* and that overexpression of the kinase causes an increase in $PIP_2$ levels *in-vivo*. In developing neurons, PPK-1 overexpression leads to growth cones that become stalled, produce ectopic membrane projections, and branched axons. Once neurons are established, PPK-1 overexpression results in progressive membrane overgrowth and degeneration during adulthood. These data suggest that overexpression of the Type I PIP kinase inhibits growth cone collapse, and that regulation of $PIP_2$ levels in established neurons may be important to maintain structural integrity and prevent neuronal degeneration.

### Keywords

PI(4,5)P2; PIP5K; Axon outgrowth; C. elegans; Neuron maintenance; Neuron degeneration

correspondence: Kim Schuske, E-mail: schuske@biology.utah.edu, David Weinkove, E-mail: d.weinkove@ucl.ac.uk.
*authors contributed equally
†present address: Babraham Institute, Babraham Research Campus, Cambridge CB2, 4AT, UK
§present address: Inositide laboratory, Paterson Institute for Cancer Research, The University of Manchester, Wilmslow Road, Withington, Manchester M20, 4BX, UK

## Introduction

Many of the actin remodeling proteins expressed in growth cones bind to the membrane lipid phosphatidylinositol 4,5 bisphosphate ($PIP_2$) including GAP-43, MARCKS, and WASP (Hartwig and Kwiatkowski, 1991; Higgs and Pollard, 2000; Laux et al., 2000; Rohatgi et al., 2000; Sechi and Wehland, 2000). Binding of these proteins to domains at the plasma membrane where $PIP_2$ is concentrated, may affect actin-mediated morphological changes (Rozelle et al., 2000). Given the dramatic cytoskeletal changes that occur during growth cone migration, it is possible that $PIP_2$ plays a role in this process.

$PIP_2$ is primarily synthesized by phosphorylation of phosphatidylinositol (4) phosphate by phosphatidylinositol phosphate 5-kinases (PIP5Ks or Type I PIP kinases) (Ishihara et al., 1996; Loijens and Anderson, 1996; Stephens et al., 1991; Whiteford et al., 1997). Studies in cultured cells have implicated PIP5Ks in the regulation of actin reorganization (Desrivieres et al., 1998; Ishihara et al., 1998; Shibasaki et al., 1997). Overexpression of the PIP5K stimulated the production of actin filaments in COS-7 cells; actin comet tails in 3T3, REF52, and mouse embryonic fibroblast cells; and F-actin coated vacuoles in Hela, 293T, and 3T3L1 adipocytes (Benesch et al., 2002; Brown et al., 2001; Galiano et al., 2002; Kanzaki et al., 2004; Rozelle et al., 2000; Shibasaki et al., 1997). In contrast, decreases in $PIP_2$ levels through inhibition of the PIP5K impaired actin remodeling (Coppolino et al., 2002; Raucher et al., 2000; Sakisaka et al., 1997). While there is no direct data indicating a role for $PIP_2$ or the PIP5K in growth cone migration, there is indirect evidence that such a role might exist. Small GTPases such as Rho and Rac, which function during growth cone migration, regulate the localization and activity of the PIP5K in non-neuronal cells and could recapitulate this function in growth cones (Brown et al., 2001; Chatah and Abrams, 2001; Chong et al., 1994; Govek et al., 2005; Honda et al., 1999; Ma et al., 1998; Tolias and Carpenter, 2000; Tolias et al., 2000). Consistent with this notion, overexpression of PIP5K in cultured neuroblastoma cells leads to retraction of neurite structures. In addition, dominant negative forms of the PIP5K prevent neurite retraction induced by semaphorin3A, Rho, and Rho kinase (ROCK) (van Horck et al., 2002; Yamazaki et al., 2002). These data suggest that disruption of PIP5K and $PIP_2$ may interfere with semaphorin and Rho-dependent growth cone collapse. However, a role for the PIP5K and $PIP_2$ in growth cone dynamics and neuron migration in a developing nervous system has never been tested.

*Caenorhabditis elegans* is an ideal organism in which to study $PIP_2$ regulated growth cone migration. First, a single PIP5K exists in the worm in contrast to mammals which have three isoforms. Second, levels of $PIP_2$ can be manipulated in the worm by overexpressing PIP5K. Third, robust growth cones are formed and can be visualized in developing GABA neurons. These growth cones migrate across the body of the worm and change morphology in response to substrates allowing for a detailed characterization of endogenous growth cone migration (Knobel et al., 1999).

In this study we characterize the *Caenorhabditis elegans* Type I PIP kinase, PPK-1. When PPK-1 is overexpressed in developing neurons, growth cones extend ectopic filopodial-like structures and fail to efficiently collapse, leading to inappropriate axonal branching. Interestingly, exposure to high levels of PPK-1 in established adult neurons causes progressive membrane overgrowth and degeneration. These data suggest that mis-regulation of PPK-1 and $PIP_2$ disrupts axon development and maintenance.

## Materials and methods

### Strains

**Mutant strains—**VC963: *ppk-1(ok1411) I / szT1 X*; + / *szT1 X*, UF66: *ppk-1(ok1411)* I; *gqIs3 [ppk-1 genomic rescue, gpb-2:GFP]* /+; *oxIs12[Punc-47:GFP, lin-15+]* X. GFP in GABA neurons: EG1306: *oxIs12[Punc-47:GFP, lin-15+] X lin-15(n765ts)* X (Knobel et al., 1999; McIntire et al., 1997). *Pppk-1* GFP reporter strain: UF70: *gqEx33[Pppk-1:GFP; lin-15+]; lin-15(n765ts)*. GFP tagged PPK-1 strain: UF60: *gqIs35[Prab-3::ppk-1::GFP, lin-15*(+)*]* IV; *lin-15(n765ts)* X. PPK-1 overexpression strains: UF64: *gqIs37[Punc-47::ppk-1; myo-2:GFP]* II; *oxIs12[Punc-47:GFP, lin-15+]* X, UF65: *gqIs25[Prab-3::ppk-1, lin-15*(+)*]*; *muIs32[Pmec-7:GFP]*, EG3361: *gqIs25[Prab-3::ppk-1, lin-15*(+)*]* I; *oxIs12[Punc-47:GFP, lin-15+]* X.

### Sequences for alignment

Putative FYVE finger-containing PI kinase, *D. melanogaster* (O96838), FYVE finger-containing PI kinase, *H. sapiens* (Q9Y2I7), FYVE finger-containing PI kinase, *M. musculus* (Q9Z1T6), PPK-3, *C. elegans* (Q9XTF8), Fab1p, *S. cerevisiae* (P34756), PPK-1, *C. elegans* (O01759), putative 1-PI4P 5-kinase, *D. melanogaster* (Q0E8Y1), skittles, *D. melanogaster* (Q7JNK2), Type Iα PI4P 5-kinase, *H. sapiens* (Q99755), Type Iγ PI4P 5-kinase, *H. sapiens* (O60331), Type Iβ PI4P 5-kinase, *H. sapiens* (O14986), Type IIα PI5P 4-kinase, *H. sapiens* (P48426), Type IIβ PI5P 4-kinase, *H. sapiens* (P78356), Type IIγ PI5P 4-kinase, *H. sapiens* (Q8TBX8), MSS4, *S. cerevisiae* (P38994), PPK-2, *C. elegans* (Q9BL73), Type Iα PI4P 5-kinase, *M. musculus* (P70182), Type Iγ PI4P 5-kinase, *M. musculus* (O70161), Type Iβ PI4P 5-kinase, *M. musculus* (P70181), Type IIα PI5P 4-kinase, *M. musculus* (O70172), Type IIβ PI5P 4-kinase, *M. musculus* (Q80XI4), Type IIγ PI5P 4-kinase, *M. musculus* (Q91XU3).

### Transgenes

**ppk-1 genomic transgene—**To make the *ppk-1* genomic rescuing transgene, a 9 kb PCR product was amplified with the primers TC3: AGATTACATTTTTGCCGCCGCAGGT and TC4: ATGGATCTGTTGAGGCATCTCTGAAGTAAA using Bristol (N2) genomic DNA as template. 5 ng/μl of PCR fragment along with 95 ng/μl of the marker plasmid *gpb-2::GFP* (van der Linden et al., 2001) was injected to create the array *qaEx2904*. The array was integrated using gamma irradiation to create the integrated array *gqIs3[ppk-1; gpb-2::GFP]*

Neuronal overexpression transgenes. The P*rab-3::PPK-1* fusions transgene was made based on a PCR based fusion technique previously described (Hobert, 2002). The following primers were used to amplify the *rab-3* promoter: GCATATTTTTTGACGACGACGACC and CATCTGAAAATAGGGCTACTGTAG and the *ppk-1* genomic region: CTATTTTCAGATGGCTTCTCGGTCCACAACA and TC4. The PCR fragments which overlap, were annealed and amplified using the internal primers: GATCTTCAGATGGGAGCAGTGG (*rab-3* 5′ internal) and GCTGCCACCAATCCTCTATTGAC to create the fused product. Similarly the P*unc-47::PPK-1* transgene was made using the primers GCCAATTTGTCCTGTGAATCG and CATCTGTAATGAAATAAATGTGACGC to amplify the *unc-47* promoter and GCGTCACATTTATTTCATTACAGATGGCTTCTCGGTCCACAACA and TC4 to amplify the *ppk-1* genomic region. The PCR fragments were annealed and amplified using the internal primers CCCGGAACAGTCGAAAGTCG and GCTGCCACCAATCCTCTATTGAC.

The GFP tagged *Prab-3*:PPK-1 transgene was made using a three way PCR based on the PCR fusion approach. The *rab-3* promoter and *ppk-1* genomic regions were amplified separately using the primers described above. A *ppk-1*:GFP fusion primer

gtgagtggtgacacacctgtcgctAGCTTGCATGCCTGCAGGTCGACT was used with the primer AAGGGCCCGTACGGCCGACTAGTAGG to amplify GFP from the plasmid pPD95.75. All three PCR products were combined and the fusion made using the primer rab-3 5′ internal (see above) and the GFP 3′ internal primer GGAAACAGTTATGTTTGGTATATTGGG. All PCR fusion products were injected at 20ng/μl with 50ng/μl lin-15+plasmid EK L15 (lin-15+)(Clark et al., 1994) into MT1642 *lin-15(n765)*. Extrachromosomal arrays were integrated by X-ray irradiation and the resulting integrant *gqIs35* was outcrossed several times using MT1642.

**Pppk-1::GFP construct—**1.9 kb of upstream *ppk-1* promoter was amplified from wild type genomic DNA using the following primers: *Pppk-1:* 5′ CGGGATCCGAGCGTCACGAGACCGAATC 3′ and *Pppk-2:* 5′ CGACCGGTCCTGTGGACCGAGAAGCCATTATC 3′. The PCR fragment was digested with BamHI and AgeI restriction enzymes and cloned into equivalent sites in the GFP vector pPD95.75. The *Pppk-1::GFP* plasmid was injected at 20 ng/μl together with 60 ng/μl of EK L15. The resulting array is *gqEx33*.

## Genetics

The *ok1411* deletion of *ppk-1* was obtained from the *C. elegans* knockout consortium. The phenotype (arrested larvae) can be rescued by expression of the *gqIs3* integrated transgene containing the entire *ppk-1* gene including 1647 bp of sequence upstream of the start codon and 677 bp downstream of the predicted 3′ untranslated region, indicating the phenotype is due to deletion of the *ppk-1* gene. Larval arrest occurs after nervous system development is complete. Due to a maternal contribution, it is not possible to accurately test the role of *ppk-1* in nervous system development using these animals.

## Antibodies

Based on the predicted C-terminal sequence of PPK-1, two peptides (CGGYRLLKKMEHTWKAILHDGD, CGGSVHNPNFYASRFLTFMTEK) were synthesized with a three amino acid (CGG) N-terminal linker. The peptides were then individually coupled to keyhole limpet hemocyanin and pooled for injection into rabbits. A similar procedure was used to raise anti PPK-2 antiserum (Weinkove et al, unpublished).

The resulting polyclonal antisera were used on Western blots at a 1:1000 dilution in PBS/Tween-20 containing 4% non-fat dry milk. The secondary antibody was swine anti-rabbit-HRP (DAKO) at a 1:2000 dilution and detected using either enhanced chemiluminescence (Amersham Pharmacia Biotech) or Supersignal West Dura Extended Duration Substrate (Pierce). The specificity of the anti PPK-1 antisera was confirmed using RNAi to deplete the recognized band. PPK-2 antisera was confirmed using a mutant (Weinkove et al, unpublished).

## Phosphocellulose method for purifying PPK-1 activity from whole worm lysates

To purify active PPK-1, a 50μl pellet of L1 larvae was used for lysis in 500 μl 1% NP-40 lysis buffer (50 mM Tris-HCl pH 8.0, 50 mM KCl, 10 mM EDTA, 1% NP-40) supplemented with protease inhibitors (complete EDTA-free tablets (Roche)) and phosphatase inhibitors (sodium fluoride; sodium orthovanadate). Disintegration of larvae was accomplished by sonication (2×10 pulses), after which the actual lysis reaction was allowed to proceed on ice for 30 minutes. Lysates were centrifuged at 14000 rpm for 30 minutes (at 4°C), after which lysates were normalized for protein concentration by making use of BioRad protein assay reagent. Supernatants were added to phosphocellulose beads. 0.5 g of phosphocellulose beads (Whatman) were activated by incubating in 20 ml of 0.5 M NaOH for 5 minutes at room temperature, after which the beads were washed 10 times in 50 ml $H_2O$ and incubated for 5 minutes in 20 ml of 0.5 M HCl. Activation of the beads was completed by washing 10 times in 50 ml $H_2O$ and 5 times in base buffer (20 mM Tris-HCl pH 7.4, 2 mM MgCl, 10% ethylene

glycol, 0.05% Tween-20, 3 mM β-mercapto-ethanol). Beads were then washed in lysis buffer and 20 mls of beads were incubated with lysate for 1-2 h at 4°C to allow efficient binding of proteins to the beads. Elution was done using varying concentrations of NaCl (0.3, 0.6, and 1 M) in base buffer. All elutions were performed twice with 100 μl of base buffer/NaCl for 5 minutes on ice. The eluted fractions were then used for PIP 5-kinase assays or for Western blotting.

### PIP 5-kinase activity assay

1 nmol of PI(4)P (Echelon Biosciences), 10 nmol of phosphatidylserine (PS; Sigma-Aldrich), and 3 nmol of phosphatidic acid (PA; Sigma-Aldrich) were prepared in micelles by drying, resuspending in water, sonicated then added to 10 μl of each elution fraction as a substrate. Next, 5 μCi [$^{32}$P]-γATP (Amersham Biosciences), together with 20 μM of "cold" ATP and PIP kinase buffer (final concentration 50 mM Tris-HCl pH 7.4, 10 mM $MgCl_2$, 1 mM EGTA, 70 mM KCl), was added to the elution fraction/substrate mix. The reaction was allowed to proceed for 20 minutes at room temperature, after which the reaction was stopped by adding 500 ml of chloroform/ methanol (1:1) containing 0.1% lipid carrier (Folch Type I extract (Sigma)). Lipids were extracted by adding 125 μl of 2.4 M HCl. The top phase was removed, and lipids were extracted again with 500 μl of theoretical upper phase (500 ml stock solution contains 235 ml methanol, 245 ml 1M HCl, and 15 ml chloroform). The bottom phase was dried down and resolved by thin layer chromotography making use of the ammonia system (8.0 ml $H_2O$, 2.0 ml ammonia, 45 ml chloroform, 35 ml methanol). The PIP and $PIP_2$ standard was generated by subjecting a HT1080 cell lysate to [32P]- γATP for 10-30 minutes at 30°C, after which lipids were extracted as described above.

### *In-vivo* $PIP_2$ labelling

Starved L1s were labeled with approximately 1 mCi [$^{32}$P]-orthophosphate (Amersham Biosciences) per sample essentially as described (Weinkove et al., 2006). Larvae were killed by the addition of 500 ml of MeOH, disrupted with acid washed glass beads, and lipids extracted as described previously (Desrivieres et al., 1998). Dried lipids were divided in half. Half was resolved by thin layer chromatography using the ammonia solvent system and using $PIP_2$ generated from purified GST-MSS4 (the *S. cerevisiae* PIP5K) as a standard (Desrivieres et al., 1998). The results were analysed using a phosphoimager. The other half of the lipids were deacylated and resolved by HPLC.

### Fluorescence microscopy

**Analysis of larval neuronal phenotypes—**Worms of the appropriate age and genotype, *oxIs12[Punc-47:GFP], gqIs37[Punc-47:PPK-1]; oxIs12, gqIs25[Prab-3:PPK-1]; oxIs12, muIs32[Pmec-7:GFP]*, and *gqIs25; muIs32*, were mounted on 3% agarose pads, paralyzed with 5 mM sodium azide in M9 under a coverslip, and imaged by epifluorescence microscopy (Nikon E800 with 60X 1.4na PlanApo) or confocal microscopy (Biorad Radiance 2000). GABA DD and VD neurons were scored for defects in axonal morphology and assigned to one of the following classes: normal commissure, prematurely terminating axon, branched axon, and prolonged growth cone. In a few cases, neurons displayed multiple phenotypes. ALM and PVC neurons were scored for abnormal projections. Any ALM projection that was longer than the average wild type projection was scored as defective.

**Longitudinal studies—**Newly hatched L1 *gqIs37[Punc-47:PPK-1]; oxIs12* worms were mounted individually on 3% agarose pads under a coverslip in 5 μl of 10 mM muscimol in M9; muscimol was used to anesthetize worms because worms recovered from these slides quickly and resumed normal behavior and growth. Images of VD and DD neurons were taken with a confocal microscope (Biorad Radiance 2000 with 60X 1.4na PlanApo). After imaging,

worms were recovered from slides and returned to small agar plates seeded with HB101. The second time point was approximately 15 hours after hatching, the third time point approximately 24 hours later, and the final time point was 24 hours later (animals were morphologically adults at this time point). In all, ten worms were imaged and all worms showed progressive phenotypes. *Prab-3:PPK-1; oxIs12* worms were imaged starting as L4 larvae (determined by vulval morphology). Animals were allowed to recover on plates seeded with HB101 placed at room temperature until the next time point. Animals were imaged as one day, two day, four day, and six day old adults. Eight worms were imaged, but only four survived to six day old adults, and all worms showed progressive phenotypes. DVB neurons were imaged independently as L2 larvae (15 hours after embryo hatching at 22°C), L4, one day, four day, and seven day old adults. Ten worms were imaged, but only five survived to become seven day old adults and all showed progressive phenotypes.

**Growth cone analysis—**Either wild type, *oxIs12*, or *gqIs37[Punc-47:PPK-1]; oxIs12* worms were picked at hatch (time 0 hrs) and maintained at either 22 or 15° C. VD growth cones extend at about 15 hours (at 22° C) or 17 hrs (15° C). Worms were mounted on 6-8 % agarose pads in 5 ul of 10 mM muscimol (Sigma) in M9. Coverslips were sealed with Vasoline to prevent the agarose pads from drying. Individual worms selected on the basis of gonad development were quickly scanned to identify suitable growth cones. Individual growth cones were imaged with a confocal microscope using a Nikon 60X 1.4na PlanApo lens at a time interval of 60-120 seconds. Duration of time lapse experiments varied from 1-4 hours.

The average time it took wild type and *Punc-47*:PPK-1 growth cones to reach the dorsal muscle, form an anvil, send a projection to the dorsal cord, and collapse was calculated. Not all migrating growth cones were imaged as they were leaving the ventral cord. Some time-lapse series start between landmark points. For this reason the time was calculated for each growth cone that went from one landmark to the next. For example, if imaging of a growth cone began after it had reached the muscle, but had not formed an anvil, then the time point between anvil formation, reaching the dorsal muscle, and growth cone collapse were calculated, but time to form the anvil was not.

High magnification time-lapse series were taken of growth cones, after anvil formation, in order to calculate membrane projection number, length, and life span at the following settings: 512×512 pixels, zoom 8 (0.05 pixels/um), 166 lines/s, laser power 1-2% (5 mW 488 line), iris 2.5-3.5, z step 0.5-1um, and time interval of 60 sec. Z stacks varied from 3-6 um. Duration of time-lapse experiments varied from 1-4 hours. For wild type, only growth cones that showed ectopic (non-dorsal) projections were used. For this reason, projection number is overestimated in wild type and the true difference between wild type and *Punc-47:PPK-1* growth cones is likely to be greater. Measurements were taken using Image J. VD and DD neurons were analyzed in both strains.

## Results

### PPK-1 is the only Type I PIP kinase in *C. elegans*

The mammalian PIP kinases are divided into three classes (Type I, Type II, and Type III) on the basis of sequence and substrate specificity. BLAST search analysis of the *C. elegans* genome identified three open reading frames with homology to mammalian PIP kinases with each gene representing a single homologue of each of the three classes (Fig. 1A). The Type I PIP kinases, also called PIP5Ks, phosphorylate phosphatidylinositol 4-phosphate (PI4P) on the 5-OH position of the inositol ring to produce PI(4,5)$P_2$ (Ishihara et al., 1996;Loijens and Anderson, 1996). In mammals, there are at least three isoforms (α, β, γ). In *C. elegans* the open reading frame F55A12.3, PPK-1, is very similar to all three isoforms of the mammalian Type I PIP kinases. Type II PIP kinases, also called PIP4Ks, phosphorylate phosphatidylinositol 5-

phosphate (PI5P) on the 4-OH position to PI(4,5)$P_2$ (Boronenkov and Anderson, 1995;Castellino et al., 1997;Itoh et al., 1998;Rameh et al., 1997). The Type II kinase is represented by the *C. elegans* open reading frame Y48G9A.8 and was named PPK-2 (Weinkove et al, unpublished). Type III PIP kinases, also called PIKfyve kinases in mammals, make a different product than Type 1 and Type II, by phosphorylating phosphatidylinositol 3-phosphate (PI3P) on the 5-OH position to make PI(3,5)$P_2$ (McEwen et al., 1999;Sbrissa et al., 2002;Sbrissa et al., 1999). The *C. elegans* open reading frame VF11C1L.1 encodes a Type III PIP kinase and is named PPK-3 (Nicot et al., 2006).

Previous studies in other systems showed that Type I PIP kinases (PIP5K) are the primary enzymes responsible for producing PI(4,5)$P_2$ at the plasma membrane of most cells (Stephens et al., 1991; Whiteford et al., 1997). PPK-1 is approximately 50% identical with Type I PIP kinases in other species. In addition, PPK-1 possesses 16 out of 22 amino acids shared between all human Type I PIP kinases in a region of the protein termed the activation loop, which has been shown to govern substrate specificity (Kunz et al., 2002). While the Type II PIP kinase can also make PI(4,5)$P_2$ *in-vitro*, the contribution of this enzyme to cellular PI(4,5)$P_2$ levels is unknown. In *C. elegans*, a deletion allele of *ppk-2* is viable and shows no gross defects or reduction in levels of $^{32}$P-orthophosphate-labeled $PIP_2$ suggesting it is not critical for $PIP_2$ production in the worm (Weinkove et al unpublished). By contrast, *ppk-1(ok1411)* deletion mutants arrest as uncoordinated larvae. The *ppk-1(ok1411)* mutant animals are likely to survive due to a maternal contribution. L4 animals fed with bacteria producing double stranded *ppk-1* RNA produce dead embryos and cosuppression of germline *ppk-1* results in sterility (Robert et al., 2005) (data not shown), suggesting *ppk*-1 has an early embryonic role.

To confirm that PPK-1 has PI4P 5-kinase activity, we purified the activity using crude fractionation of a detergent lysate of *C. elegans* (Fig. 1B). Specifically, lysate was bound to activated phosphocellulose beads, washed and fractions were eluted using increasing concentrations of sodium chloride. Fractions were assayed for PI4P 5-kinase activity and for PPK-1 protein by Western blotting. These experiments showed that the 0.3M NaCl fraction contained the highest PI4P 5-kinase activity and had the majority of PPK-1 protein. In contrast, the Type II PIP kinase (PPK-2) was primarily found in the 0.6M NaCl fraction, which showed minimal PI4P 5-kinase activity. Taken together our data suggest PPK-1 is the main PIP kinase for PI(4,5)$P_2$ production in *C. elegans*.

## *ppk-1* is highly expressed in the nervous system

To determine the endogenous expression pattern of *ppk-1*, GFP was expressed under the control of the *ppk-1* promoter. 1.9 kb of sequence upstream of the *ppk-1* start codon was PCR amplified and fused to GFP. Examination of the resulting transgenic animals revealed that *ppk-1* is broadly expressed in early embryos (data not shown). In adults, *ppk-1* is expressed at high levels throughout the nervous system as well as in the spermatheca, hypodermal seam cells, and distal tip cell of the gonad (Figs. 2 A-E). Lower expression is seen in the intestine, gonad, and body wall muscle. The high level of expression of *ppk-1* in the nervous system suggests it has an important role in this tissue.

Studies in other systems demonstrated that the Type I PIP kinase is primarily localized at the plasma membrane. To determine where the *C. elegans* kinase is localized within neurons, PPK-1 protein with GFP fused to the C-terminus was expressed under the control of a pan-neuronal promoter for the *rab-3* gene (Nonet et al., 1997). Similar to the vertebrate Type 1 kinase, the PPK-1:GFP fusion protein can localize to the plasma membrane (Figs. 2 F, G).

Interestingly, animals expressing the PPK-1:GFP fusion protein are uncoordinated. A similar uncoordinated phenotype is observed in animals overexpressing an untagged PPK-1 under the *rab-3* promoter (Jospin et al., 2007) as well as worms expressing an untagged PPK-1 under

the endogenous *ppk-1* promoter. This suggests that overexpression of PPK-1 in neurons leads to nervous system disruption.

## Overexpression of PPK-1 leads to increased $PIP_2$

To determine if overexpression of PPK-1 can increase $PIP_2$ levels in *Prab-3*::PPK-1 animals, we labeled L1 larvae with $^{32}$P-orthophosphate and assayed for the presence of $PIP_2$. Lipids were extracted, separated by thin layer chromatography and quantified by phosphoimager. In parallel, lipids were deacetylated and analyzed by HPLC. Levels of $PIP_2$ as a proportion of total labeled phospholipid were increased approximately 40% in animals overexpressing *ppk-1* in neurons compared to controls (Fig. 3A). Given that the *rab-3* promoter is only active in neuronal cells, the cellular increase in $PIP_2$ levels in worms overexpressing PPK-1 are likely to be considerable suggesting it is possible to override feedback mechanisms that are thought to maintain stable levels of $PIP_2$ in the cell (Ling et al., 2006).

## Mature neurons are susceptible to PPK-1 overexpression

Why are animals overexpressing PPK-1 uncoordinated? $PIP_2$ is an important regulator of many cellular processes including membrane trafficking, actin polymerization, and signal transduction. In neurons of mice lacking PI5PKγ, synaptic vesicle recycling is disrupted (Di Paolo et al., 2004). However, the effect of overexpressing the kinase in an endogenous nervous system has not been previously tested. To determine if the structure of the nervous system is normal in *Prab-3*:PPK-1 animals, we analyzed a subset of motor and mechanosensory neurons.

The DD and VD motor neurons were analyzed using a construct expressing GFP under the GABA specific promoter *unc-47*. The GABA nervous system in *C. elegans* consists of 26 out of 302 total neurons. Nineteen of these are the VD and DD motor neurons whose cell bodies are located on the ventral side of the worm. Axons from these neurons migrate circumferentially across the body of the worm until they reach the dorsal side where they form part of the dorsal nerve cord. A pair of longitudinal mechanosensory neurons, ALM left and right, were analyzed using a construct expressing GFP under the *mec-7* promoter (Hamelin et al., 1992) (R. Korswagen, personal communication). The cell body of these neurons is located near the anterior, dorsal side of the worm. The ALM neuron sends a projection towards the head and occasionally has a short projection that is sent towards the posterior.

Overexpression of PPK-1 disrupted both motor neuron and mechanosensory neuron structure (Figs. 3B, C). Interestingly, a quantitative analysis in which animals were imaged at different stages of development showed that the number of defects increased as an animal aged. Specifically, 12% of animals in early larval stages (5, 15, and 24 hours after hatching) had GABA neuron pathfinding or axon branching defects, this increased to 54% in L4 larvae and 90% in young adults. Only 8% of wild type adults showed similar defects (Fig. 3B). A similar age-dependent accumulation of defects was seen in mechanosensory neurons (Fig. 3C). Thus, overexpression of PPK-1 appears to disrupt neuron maintenance.

To more thoroughly characterize neuronal maintenance in *Prab-3*::PPK-1 animals, a longitudinal analysis was performed. Individual animals were imaged multiple times, starting as L4 larvae, and ending as six-day old adults. The analysis showed that there is a dramatic progression of defects as *Prab-3*:PPK-1 adult animals age (Figs. 4A-D). Three main defects were observed. First, ectopic growths were found to initiate either from existing axons, or from the ventral nerve cord (Fig. 4A). No obvious growth initiated from the dorsal nerve cord. Once an ectopic growth was initiated, there appeared to be no clear direction of growth. Rather, as the animals aged the projections continued to extend in random orientations sometimes leading to a tangled mass of axon. Second, some existing axons became increasingly thin and started to form membrane blebs as the animals aged (Fig. 4B). While many of the axons remained

barely visible in six-day old adult animals, some of the axons were no longer visible by this stage suggesting they had degenerated. Third, ectopic projections initiated from some cell bodies, most evident in the isolated neuron DVB in the tail of the worm (Fig. 4C). The number of projections, length of projections, and branches from a given projection all increase as an adult aged (Fig. 4D). Finally, both the ventral and dorsal nerve cords became increasingly defasciculated (data not shown). Thus, overexpression of PPK-1 leads to progressive overgrowth and degeneration of established neurons.

### Overexpression of PPK-1 in developing neurons inhibits growth cone collapse

The ectopic membranous projections observed in adult neurons suggest that overexpression of PPK-1 is disrupting the structure of the neuron cytoskeleton. However, during neuron development the cystoskeleton is constantly changing in response to environmental cues. Why are there no defects in developing neurons when PPK-1 is overexpressed? One possibility is that the larval nervous system is resistant to high levels of PPK-1 while the adult nervous system is sensitive. A second and more likely possibility is that PPK-1 or $PIP_2$ is not expressed at high enough levels in early larvae in the *Prab-3*::PPK-1 animals to disrupt development.

We attempted to look at *ppk-1(ok1411)* mutants to determine if PPK-1 is required for neuron development. GABA neurons in maternally wild type *ppk-1(ok1411)* zygotic mutant larvae appear to grow out normally, but the axons look slightly thinner and wavier than axons in wild type controls (data not shown). Given the maternal rescue observed in the mutants, it is likely that PPK-1 function is still present in these animals and precludes analysis of *ppk-1* loss-of -function phenotypes at this developmental stage.

To determine if overexpression of PPK-1 can disrupt neuron development, we expressed *ppk-1* using the *unc-47* promoter which was previously shown to be turned on in the DD and VD neurons prior to axon outgrowth (Knobel et al., 1999). Similar to *Prab-3*:PPK-1 animals, *Punc-47*:PPK-1 animals show defects in neuron structure, however the defects start earlier: 81%, 90%, and 100% of larvae 5, 15 and 24 hours after embryonic hatching respectively show premature axon termination, axon branching, and prolonged growth cone defects (Fig. 5). This is in contrast to *Prab-3*:PPK-1 animals in which only 12% of larvae at these stages had defects.

To determine if the defects are due to disruption of growth cone behavior during migration, we used time-lapse imaging to analyze individual growth cones in wild type and *Punc-47*::PPK-1 animals. Wild type GABA growth cones exhibit morphological changes as they encounter new substrates (Figs. 6A, B, Sup. movies 1, 2). During migration across the hypodermis the growth cone forms a broad lamellipodial-like structure with multiple filopodial-like projections. When the growth cone encounters the dorsal muscle, it forms an anvil shape and then sends out fingers between the muscle/hypodermal attachment structures. Usually a single finger extends beyond the muscle and migrates towards the dorsal nerve cord. Once the finger reaches the dorsal cord, the anvil immediately collapses and a new growth cone forms in order to extend along the dorsal cord (Knobel et al., 1999).

Time lapse analysis of animals overexpressing PPK-1 indicate that growth cones migrate at normal rates across the hypodermis, form anvils at the muscle boundary and send fingers towards the dorsal nerve cord. However, two main defects were observed: growth cones fail to properly collapse, and they send out ectopic membrane projections. 58% of growth cones that make it to the dorsal body wall muscle boundary fail to collapse (Figs. 6A, B, Sup. movie 3). In the defective growth cones, the length of time spent at the muscle boundary prior to collapse ranged between 57 minutes and greater than 3 hours (at which time the analysis was terminated). This is in contrast to wild type growth cones which collapse in less than two minutes of reaching the dorsal cord. Occasionally, defective *Punc-47*:PPK-1 growth cones reached the dorsal nerve cord, and partial, but not complete collapse of the growth cone was

observed (Fig. 6B, Sup. movie 3). Thus, overexpression of PPK-1 does not appear to prevent a collapse signal from being received, but instead may stabilize the structure of the growth cone.

Once a wild type growth cone reaches the dorsal muscle, an anvil shape forms, and most membrane projections are sent towards the dorsal cord. In contrast, while growth cones in *Punc-47*::PPK-1 animals form anvils and send projections towards the dorsal cord, many also send out ectopic projections from other surfaces of the growth cone, as well as occasionally from the axon (Fig. 6B, Sup. movie 3). To determine if projection number, length, and lifespan (time from extension to retraction) are affected by overexpression of PPK-1, we analyzed *in-vivo* growth cone behavior at the muscle boundary using high magnification time-lapse imaging. The number, length and life span of ectopic projections, excluding dorsal projections, were compared between wild type and *Punc-47:*PP*K-1* growth cones. Growth cones in animals overexpressing PPK-1 display more projections (wild type: 2.3 ± 0.6 SEM n=4, *Punc-47:PPK-1:* 11.5 ± 3.6 SEM n=4, unpaired T- test p=0.04), the projections were longer at their maximum length (wild type: 1.4 μm ± 0.2 SEM n=9, *Punc-47:PPK-1:* 3.7 μm ± 0.4 SEM n=46, p= 0.008), and the period encompassing growth and retraction was longer when compared to wild type (wild type: 2.6 min. ± 0.7 SEM n= 9, *Punc-47:PPK-1:* 14.9 min ± 2.6 SEM n=46, p=0.04). In summary, time-lapse imaging experiments indicate that growth cones overexpressing *ppk-1* often fail to collapse at the dorsal muscle and send out abnormal ectopic filopodial-like projections.

How do growth cone defects in animals overexpressing PPK-1 affect the final structure of the nervous system? To address this question, a longitudinal analysis was performed in which single animals were imaged at multiple developmental stages. We found that the majority of neurons eventually make their way to the dorsal cord. However, the route taken is often indirect. For example, growth cones, which appear to be stuck at the dorsal muscle boundary, often send lateral branches along this boundary. The branches remain as the animal ages and occasionally can form secondary projections that also migrate to the dorsal cord (Figs. 7A, B). Secondary branches not only appear from stalled growth cones, but also extend from other locations along the axon and from the ventral cord, suggesting that when *ppk-1* is overexpressed developing neurons are plastic.

## Discussion

$PI(4,5)P_2$ is an important lipid that has been implicated in diverse biological processes including membrane trafficking, actin polymerization, protein localization, and cell signaling. Most studies of $PIP_2$ and PIP5Ks have been performed in cultured cell systems or in *in-vitro* biochemical assays. In this study we characterize the *C. elegans* PIP5K and show that this kinase can generate $PIP_2$ *in-vitro*. Overexpression of the kinase in neurons leads to uncoordinated locomotion, which is likely to be partially due to defects in the structure of the nervous system. Overexpression of PPK-1 in developing neurons causes specific defects in growth cone migration, while overexpression in established neurons causes abnormal growth and eventual degeneration. Since overexpression of PPK-1 throughout the nervous system can lead to increased $^{32}P$ –labelled $PIP_2$, this suggests the effect is due to increased $PIP_2$ or its byproducts.

One of the main phenotypes we observe when PPK-1 is overexpressed in developing or mature neurons is an increase in the number of membranous projections. Our data is consistent with previous studies that overexpress PIP5K in non-neuronal cultured cells. Overexpression of PIP5K in multiple cell types increase actin based cytoskeletal structures (Benesch et al., 2002; Brown et al., 2001; Galiano et al., 2002; Kanzaki et al., 2004; Rozelle et al., 2000; Shibasaki et al., 1997). However, our data appears to contradict studies conducted in cultured

neuroblastoma cells which showed that overexpression of PIP5K causes retraction of neurite structures (van Horck et al., 2002; Yamazaki et al., 2002). One possible explanation for the difference between our studies is the environments in which the neurons are migrating. For example, the adhesive environment in an intact animal is likely to be very different from a neuron grown in culture. In addition, the network of intracellular signaling components in a *C. elegans* motor neuron is likely to differ from a neuroblastoma cell. Finally, it is possible that individual isoforms of mammalian PIP5Ks play specific roles in neurite extension and maintenance (Giudici et al., 2004). Any one of these differences could determine how the cells respond to high levels of the kinase. Alternatively, the levels of PIP5K that each cell is exposed to may not be equivalent in the different experimental systems.

What does PPK-1 overexpression reveal about the potential role of $PIP_2$ in growth cone migration? It is surprising that growth cones in animals overexpressing PPK-1 have such a specific defect. While the *unc-47* promoter turns on quickly after the DD and VD neurons are born, it may take some time for PPK-1 and $PIP_2$ levels to reach a critical concentration in the developing neuron. This could be one reason that growth cones show a preferential defect at the muscle boundary. However, since many of the growth cones that make it to the muscle boundary show ectopic projections and a failure to collapse, it is likely that these are the processes that are most sensitive to high levels of PPK-1. High levels of $PIP_2$ could inhibit actin capping proteins such as cofilin and gelsolin. Inhibition of these proteins might stabilize the growth cone structure and possibly cause an increase in membrane projections. Interestingly, hippocampal cells cultured from gelsolin knockout mice do show an increased number of filopodia (Lu et al., 1997), a phenotype similar to that observed in neurons overexpressing PPK-1, suggesting gelsolin could be inhibited by $PIP_2$ in our system.

What does overexpression of PPK-1 in adult neurons suggest about the role of $PIP_2$ in the adult nervous system? Previous studies suggest that an increase in $PIP_2$ levels at sites of endocytosis in the absence of the phosphatidylinositol phosphatase, synaptojanin, disrupts synaptic vesicle recycling (Cremona et al., 1999; Dickman et al., 2005; Harris et al., 2000; Verstreken et al., 2003). In *C. elegans*, synaptojanin mutants do not appear to have a defect in neuron structure (our unpublished observation). By contrast, overexpression of PPK-1 in adult neurons disrupts neuron structure and eventually causes neuron degeneration. The disparity in phenotypes may be due to the region within a cell that is exposed to the increased $PIP_2$. In synaptojanin mutants, the increase in $PIP_2$ is thought to be confined to sites of endocytosis, while overexpression of PPK-1 is expected to increase $PIP_2$ throughout the neuron plasma membrane. The difference in phenotypes suggest that by altering the subcellular levels of $PIP_2$ in a genetic system, it may eventually be possible dissect the cellular functions of this important lipid *in-vivo*.

## Supplementary Material

Refer to Web version on PubMed Central for supplementary material.

## Acknowledgments

We would like to thank R. Korswagen for *muIs32*, the *C. elegans* knockout consortium for *ppk-1(ok1141)*, J. Weis and M. Prestgard-Duke for technical assistance, M. Horner, K. Knobel, and A. Ada-Nguema for comments on the manuscript, and J. Halstead, D. Jones, and E. Jorgensen for advice. This research was funded by grants from the National Institutes of Health (NS048391) and the Lowe Syndrome Association and the Lowe Syndrome Trust to K.S., the H. Neilson Foundation, the McKnight Endowment Fund for Neuroscience, and NIH (NS060275) to M. B., the Netherlands Cancer Institute (D.W., N.D., T.C.), the Wellcome Trust (D.W. and F.C.), and a short term fellowship from the Human Frontiers Science Program to D.W.

## References


Benesch S, Lommel S, Steffen A, Stradal TE, Scaplehorn N, Way M, Wehland J, Rottner K. Phosphatidylinositol 4,5-biphosphate (PIP2)-induced vesicle movement depends on N-WASP and involves Nck, WIP, and Grb2. J Biol Chem 2002;277:37771–6. [PubMed: 12147689]

Boronenkov IV, Anderson RA. The sequence of phosphatidylinositol-4-phosphate 5-kinase defines a novel family of lipid kinases. J Biol Chem 1995;270:2881–4. [PubMed: 7852364]

Brown FD, Rozelle AL, Yin HL, Balla T, Donaldson JG. Phosphatidylinositol 4,5-bisphosphate and Arf6-regulated membrane traffic. J Cell Biol 2001;154:1007–17. [PubMed: 11535619]

Castellino AM, Parker GJ, Boronenkov IV, Anderson RA, Chao MV. A novel interaction between the juxtamembrane region of the p55 tumor necrosis factor receptor and phosphatidylinositol-4-phosphate 5-kinase. J Biol Chem 1997;272:5861–70. [PubMed: 9038203]

Chatah NEH, Abrams CS. G-protein-coupled receptor activation induces the membrane translocation and activation of phosphatidylinositol-4-phsophate 5-kinase Iα by a rac- and rho-dependent pathway. J Biol Chem 2001;276:34059–34065. [PubMed: 11431481]

Chong LD, Traynor-Kaplan A, Bokoch GM, Schwartz MA. The small GTP-binding protein Rho regulates a phosphatidylinositol 4-phosphate 5-kinase in mammalian cells. Cell 1994;79:507–13. [PubMed: 7954816]

Clark SG, Lu X, Horvitz HR. The *Caenorhabditis elegans* locus *lin-15*, a negative regulator of a tyrosine kinase signaling pathway, encodes two different proteins. Genetics 1994;137:987–997. [PubMed: 7982579]

Coppolino MG, Dierckman R, Loijens J, Collins RF, Pouladi M, Jongstra-Bilen J, Schreiber AD, Trimble WS, Anderson R, Grinstein S. Inhibition of phosphatidylinositol-4-phosphate 5-kinase Ialpha impairs localized actin remodeling and suppresses phagocytosis. J Biol Chem 2002;277:43849–57. [PubMed: 12223494]

Cremona O, Di Paolo G, Wenk M, Luthi A, Kim WT, Takei K, Daniell L, Nemoto Y, Shears SB, Flavell RA, McCormick DA, De Camilli P. Essential role of phosphoinositide metabolism in synaptic vesicle recycling. Cell 1999;99:179–188. [PubMed: 10535736]

Desrivieres S, Cooke FT, Parker PJ, Hall MN. MSS4, a phosphatidylinositol-4-phosphate 5-kinase required for organization of the actin cytoskeleton in Saccharomyces cerevisiae. J Biol Chem 1998;273:15787–93. [PubMed: 9624178]

Di Paolo G, Moskowitz HS, Gipson K, Wenk MR, Voronov S, Obayashi M, Flavell R, Fitzsimonds RM, Ryan TA, De Camilli P. Impaired PtdIns(4,5)P2 synthesis in nerve terminals produces defects in synaptic vesicle trafficking. Nature 2004;431:415–22. [PubMed: 15386003]

Dickman DK, Horne JA, Meinertzhagen IA, Schwarz TL. A slowed classical pathway rather than kiss-and-run mediates endocytosis at synapses lacking synaptojanin and endophilin. Cell 2005;123:521–33. [PubMed: 16269341]

Galiano FJ, Ulug ET, Davis JN. Overexpression of murine phosphatidylinositol 4-phosphate 5-kinase type Ibeta disrupts a phosphatidylinositol 4,5 bisphosphate regulated endosomal pathway. J Cell Biochem 2002;85:131–45. [PubMed: 11891857]

Giudici ML, Emson PC, Irvine RF. A novel neuronal-specific splice variant of Type I phosphatidylinositol 4-phosphate 5-kinase isoform gamma. Biochem J 2004;379:489–96. [PubMed: 14741049]

Govek EE, Newey SE, Van Aelst L. The role of the Rho GTPases in neuronal development. Genes Dev 2005;19:1–49. [PubMed: 15630019]

Hamelin M, Scott IM, Way JC, Culotti JG. The mec-7 beta-tubulin gene of Caenorhabditis elegans is expressed primarily in the touch receptor neurons. Embo J 1992;11:2885–93. [PubMed: 1639062]

Harris TW, Hartwieg E, Horvitz HR, Jorgensen EM. Mutations in synaptojanin disrupt synaptic vesicle recycling. J Cell Biol 2000;150:589–600. [PubMed: 10931870]

Hartwig JH, Kwiatkowski DJ. Actin-binding proteins. Curr Opin Cell Biol 1991;3:87–97. [PubMed: 1854489]

Higgs HN, Pollard TD. Activation by Cdc42 and PIP(2) of Wiskott-Aldrich syndrome protein (WASp) stimulates actin nucleation by Arp2/3 complex. J Cell Biol 2000;150:1311–20. [PubMed: 10995437]

Hobert O. PCR fusion-based approach to create reporter gene constructs for expression analysis in transgenic C. elegans. Biotechniques 2002;32:728–30. [PubMed: 11962590]

Honda A, Nogami M, Yokozeki T, Yamazaki M, Nakamura H, Watanabe H, Kawamoto K, Nakayama K, Morris AJ, Frohman MA, Kanaho Y. Phosphatidylinositol 4-phosphate 5-kinase alpha is a downstream effector of the small G protein ARF6 in membrane ruffle formation. Cell 1999;99:521–32. [PubMed: 10589680]

Ishihara H, Shibasaki Y, Kizuki N, Katagiri H, Yazaki Y, Asano T, Oka Y. Cloning of cDNAs encoding two isoforms of 68-kDa type I phosphatidylinositol-4-phosphate 5-kinase. J Biol Chem 1996;271:23611–4. [PubMed: 8798574]

Ishihara H, Shibasaki Y, Kizuki N, Wada T, Yazaki Y, Asano T, Oka Y. Type I phosphatidylinositol-4-phosphate 5-kinases. Cloning of the third isoform and deletion/substitution analysis of members of this novel lipid kinase family. J Biol Chem 1998;273:8741–8. [PubMed: 9535851]

Itoh T, Ijuin T, Takenawa T. A novel phosphatidylinositol-5-phosphate 4-kinase (phosphatidylinositol-phosphate kinase IIgamma) is phosphorylated in the endoplasmic reticulum in response to mitogenic signals. J Biol Chem 1998;273:20292–9. [PubMed: 9685379]

Jospin M, Watanabe S, Joshi D, Young S, Haming K, Thacker C, Snutch TP, Jorgensen EM, Schuske K. UNC-80 and the NCA Ion Channels Contribute to Endocytosis Defects in Synaptojanin Mutants. Curr Biol. 200710.1016/j.cub.2007.08.036

Kanzaki M, Furukawa M, Raab W, Pessin JE. Phosphatidylinositol 4,5-bisphosphate regulates adipocyte actin dynamics and GLUT4 vesicle recycling. J Biol Chem 2004;279:30622–33. [PubMed: 15123724]

Knobel KM, Jorgensen EM, Bastiani MJ. Growth cones stall and collapse during axon outgrowth in Caenorhabditis elegans. Development 1999;126:4489–98. [PubMed: 10498684]

Kunz J, Fuelling A, Kolbe L, Anderson RA. Stereo-specific substrate recognition by phosphatidylinositol phosphate kinases is swapped by changing a single amino acid residue. J Biol Chem 2002;277:5611–9. [PubMed: 11733501]

Laux T, Fukami K, Thelen M, Golub T, Frey D, Caroni P. GAP43, MARCKS, and CAP23 modulate PI(4,5)P(2) at plasmalemmal rafts, and regulate cell cortex actin dynamics through a common mechanism. J Cell Biol 2000;149:1455–72. [PubMed: 10871285]

Ling K, Schill NJ, Wagoner MP, Sun Y, Anderson RA. Movin' on up: the role of PtdIns(4,5)P(2) in cell migration. Trends Cell Biol 2006;16:276–84. [PubMed: 16616849]

Loijens JC, Anderson RA. Type I phosphatidylinositol-4-phosphate 5-kinases are distinct members of this novel lipid kinase family. J Biol Chem 1996;271:32937–43. [PubMed: 8955136]

Lu M, Witke W, Kwiatkowski DJ, Kosik KS. Delayed retraction of filopodia in gelsolin null mice. J Cell Biol 1997;138:1279–87. [PubMed: 9298983]

Ma L, Cantley LC, Janmey PA, Kirschner MW. Corequirement of specific phosphoinositides and small GTP-binding protein Cdc42 in inducing actin assembly in Xenopus egg extracts. J Cell Biol 1998;140:1125–36. [PubMed: 9490725]

McEwen RK, Dove SK, Cooke FT, Painter GF, Holmes AB, Shisheva A, Ohya Y, Parker PJ, Michell RH. Complementation analysis in PtdInsP kinase-deficient yeast mutants demonstrates that Schizosaccharomyces pombe and murine Fab1p homologues are phosphatidylinositol 3-phosphate 5-kinases. J Biol Chem 1999;274:33905–12. [PubMed: 10567352]

McIntire SL, Reimer RJ, Schuske K, Edwards RH, Jorgensen EM. Identification and characterization of the vesicular GABA transporter. Nature 1997;389:870–6. [PubMed: 9349821]

Nicot AS, Fares H, Payrastre B, Chisholm AD, Labouesse M, Laporte J. The phosphoinositide kinase PIKfyve/Fab1p regulates terminal lysosome maturation in Caenorhabditis elegans. Mol Biol Cell 2006;17:3062–74. [PubMed: 16801682]

Nonet ML, Staunton JE, Kilgard MP, Fergestad T, Hartwieg E, Horvitz HR, Jorgensen EM, Meyer BJ. Caenorhabditis elegans rab-3 mutant synapses exhibit impaired function and are partially depleted of vesicles. J Neurosci 1997;17:8061–73. [PubMed: 9334382]

Rameh LE, Tolias KF, Duckworth BC, Cantley LC. A new pathway for synthesis of phosphatidylinositol-4,5-bisphosphate. Nature 1997;390:192–6. [PubMed: 9367159]

Raucher D, Stauffer T, Chen W, Shen K, Guo S, York JD, Sheetz MP, Meyer T. Phosphatidylinositol 4,5-bisphosphate functions as a second messenger that regulates cytoskeleton-plasma membrane adhesion. Cell 2000;100:221–8. [PubMed: 10660045]

Robert VJ, Sijen T, van Wolfswinkel J, Plasterk RH. Chromatin and RNAi factors protect the C. elegans germline against repetitive sequences. Genes Dev 2005;19:782–7. [PubMed: 15774721]

Rohatgi R, Ho HY, Kirschner MW. Mechanism of N-WASP activation by CDC42 and phosphatidylinositol 4, 5- bisphosphate. J Cell Biol 2000;150:1299–310. [PubMed: 10995436]

Rozelle AL, Machesky LM, Yamamoto M, Driessens MH, Insall RH, Roth MG, Luby-Phelps K, Marriott G, Hall A, Yin HL. Phosphatidylinositol 4,5-bisphosphate induces actin-based movement of raft-enriched vesicles through WASP-Arp2/3. Curr Biol 2000;10:311–20. [PubMed: 10744973]

Sakisaka T, Itoh T, Miura K, Takenawa T. Phosphatidylinositol 4,5-bisphosphate phosphatase regulates the rearrangement of actin filaments. Mol Cell Biol 1997;17:3841–9. [PubMed: 9199318]

Sbrissa D, Ikonomov OC, Deeb R, Shisheva A. Phosphatidylinositol 5-phosphate biosynthesis is linked to PIKfyve and is involved in osmotic response pathway in mammalian cells. J Biol Chem 2002;277:47276–84. [PubMed: 12270933]

Sbrissa D, Ikonomov OC, Shisheva A. PIKfyve, a mammalian ortholog of yeast Fab1p lipid kinase, synthesizes 5-phosphoinositides. Effect of insulin. J Biol Chem 1999;274:21589–97. [PubMed: 10419465]

Sechi AS, Wehland J. The actin cytoskeleton and plasma membrane connection: PtdIns(4,5)P(2) influences cytoskeletal protein activity at the plasma membrane. J Cell Sci 2000;113(Pt 21):3685–95. [PubMed: 11034897]

Shibasaki Y, Ishihara H, Kizuki N, Asano T, Oka Y, Yazaki Y. Massive actin polymerization induced by phosphatidylinositol-4- phosphate 5-kinase in vivo. J Biol Chem 1997;272:7578–81. [PubMed: 9065410]

Stephens LR, Hughes KT, Irvine RF. Pathway of phosphatidylinositol(3,4,5)-trisphosphate synthesis in activated neutrophils. Nature 1991;351:33–9. [PubMed: 1851250]

Tolias K, Carpenter CL. In vitro interaction of phosphoinositide-4-phosphate 5-kinases with Rac. Methods Enzymol 2000;325:190–200. [PubMed: 11036604]

Tolias KF, Hartwig JH, Ishihara H, Shibasaki Y, Cantley LC, Carpenter CL. Type Ialpha phosphatidylinositol-4-phosphate 5-kinase mediates Rac-dependent actin assembly. Curr Biol 2000;10:153–6. [PubMed: 10679324]

van der Linden AM, Simmer F, Cuppen E, Plasterk RH. The G-protein beta-subunit GPB-2 in Caenorhabditis elegans regulates the G(o)alpha-G(q)alpha signaling network through interactions with the regulator of G-protein signaling proteins EGL-10 and EAT-16. Genetics 2001;158:221–35. [PubMed: 11333232]

van Horck FP, Lavazais E, Eickholt BJ, Moolenaar WH, Divecha N. Essential role of type I(alpha) phosphatidylinositol 4-phosphate 5-kinase in neurite remodeling. Curr Biol 2002;12:241–5. [PubMed: 11839279]

Verstreken P, Koh TW, Schulze KL, Zhai RG, Hiesinger PR, Zhou Y, Mehta SQ, Cao Y, Roos J, Bellen HJ. Synaptojanin is recruited by endophilin to promote synaptic vesicle uncoating. Neuron 2003;40:733–48. [PubMed: 14622578]

Weinkove D, Halstead JR, Gems D, Divecha N. Long-term starvation and ageing induce AGE-1/PI 3-kinase-dependent translocation of DAF-16/FOXO to the cytoplasm. BMC Biol 2006;4:1. [PubMed: 16457721]

Whiteford CC, Brearley CA, Ulug ET. Phosphatidylinositol 3,5-bisphosphate defines a novel PI 3-kinase pathway in resting mouse fibroblasts. Biochem J 1997;323(Pt 3):597–601. [PubMed: 9169590]

Yamazaki M, Miyazaki H, Watanabe H, Sasaki T, Maehama T, Frohman MA, Kanaho Y. Phosphatidylinositol 4-phosphate 5-kinase is essential for ROCK-mediated neurite remodeling. J Biol Chem 2002;277:17226–30. [PubMed: 11877391]

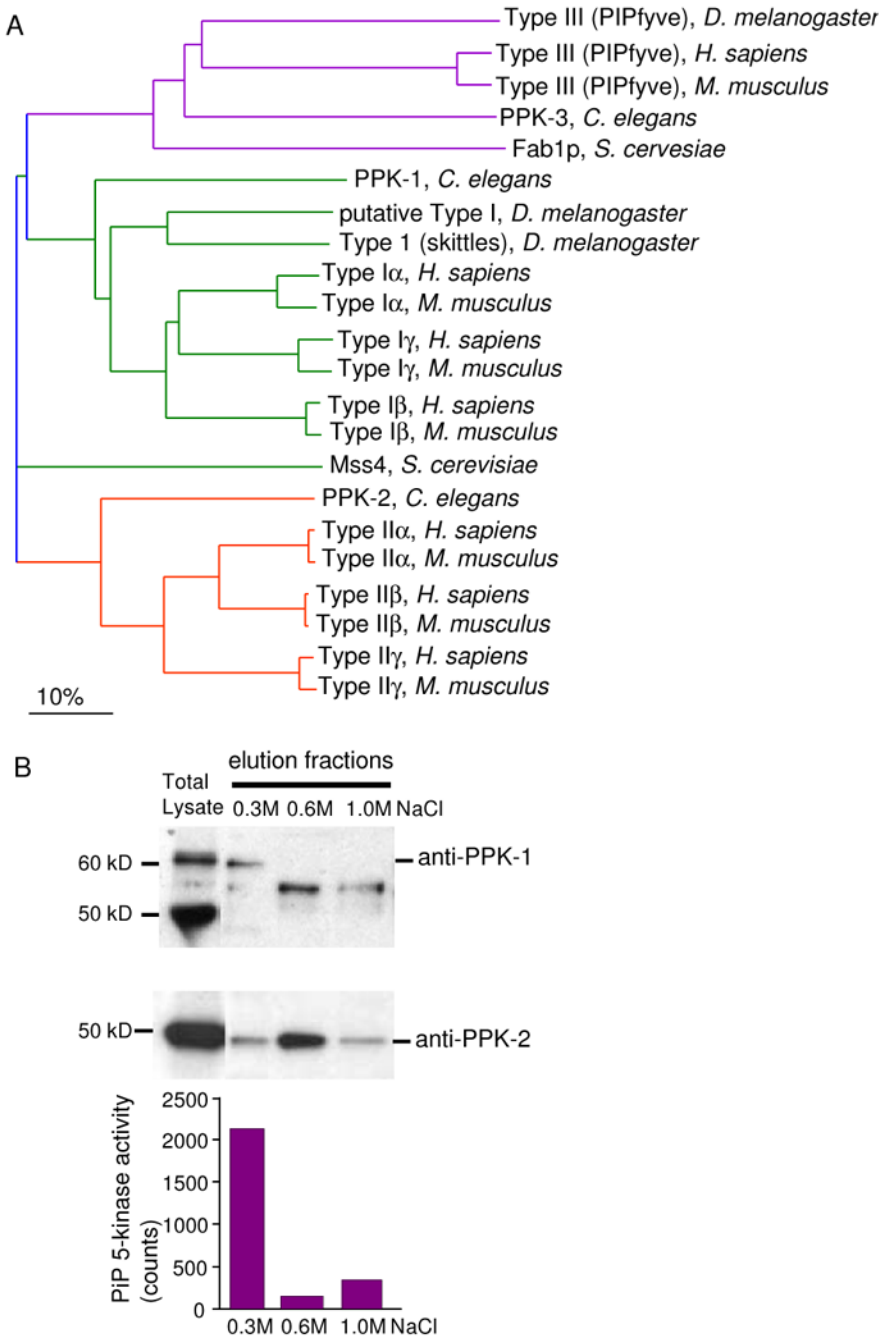


**Figure 1.**

A single Type 1 PIP kinase is present in *C. elegans* and has PIP 5-kinase activity. (A) A Guide Tree showing the interrelatedness of the PIP kinases across humans, mice, *C. elegans*, *Drosophila melanogaster* and *S. cerevisiae*. The sequences from Swiss prot (The mouse PIP kinase nomenclature has been corrected to follow the human designations) and the alignment was performed using AlignX in Vector NTI, Types I, II and III PIP kinases are color coded. (B) PPK-1 purified from lysates of starved L1s using phosphocellulose beads. Fractions were assayed for 5-kinase activity using PI4P as a substrate. PPK-1 is present in the 0.3M NaCl as assessed by kinase activity and Western blotting. PPK-2 is primarily found in the 0.6M fraction. The specificity of the anti PPK-1 antisera was confirmed using RNAi to deplete the 60kD

recognized band (data not shown). The 50 and 55kD bands were not affected by RNAi against *ppk-1*, suggesting these antibodies are not specific to the protein. PPK-2 antisera was confirmed using a mutant (Weinkove et al, unpublished).

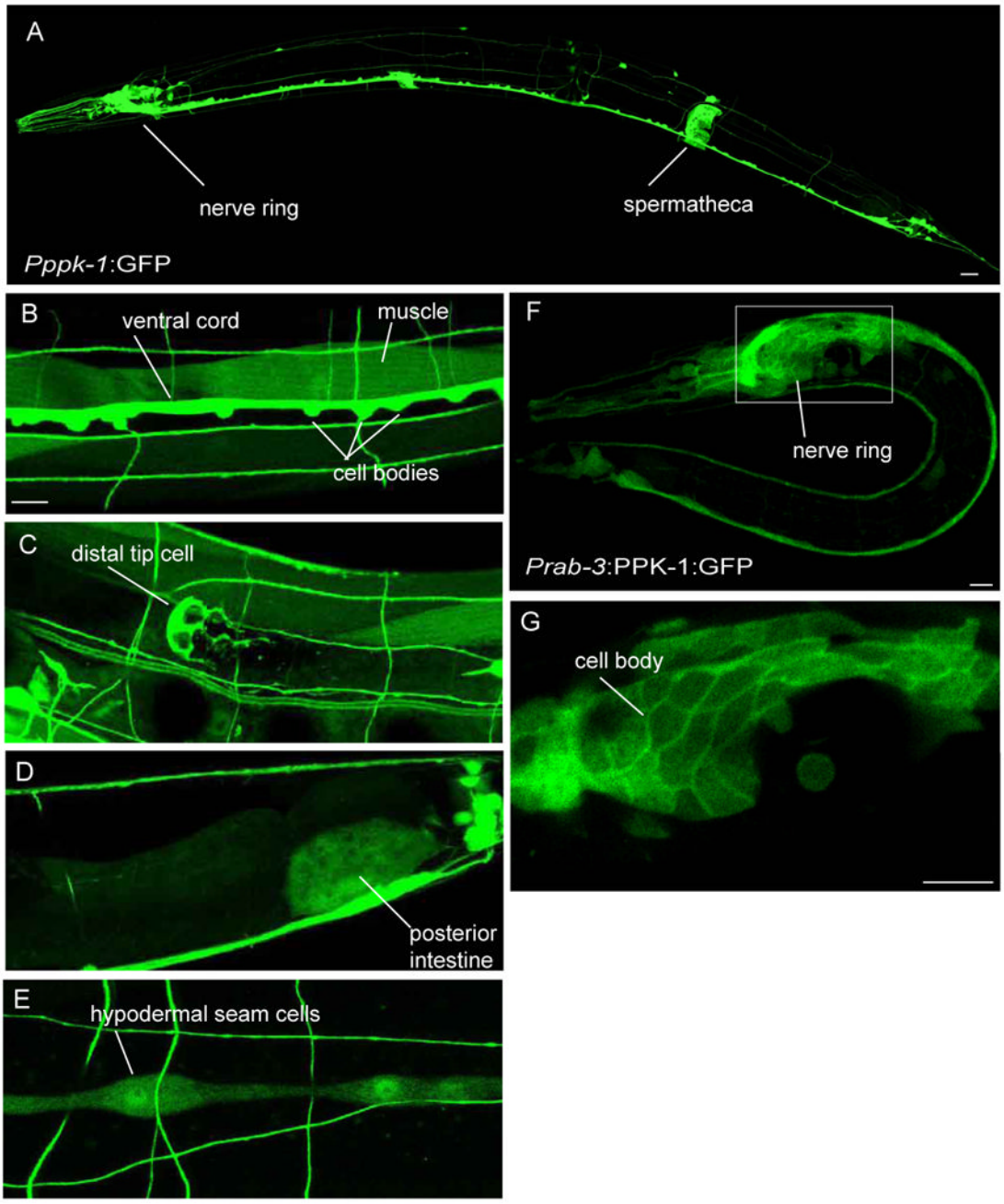


**Figure 2.**

*ppk-1* is expressed at high levels in the nervous system and localizes to the plasma membrane. (A-E) Cellular expression of *ppk-1*. *ppk-1* is expressed in multiple tissues including neurons, spermatheca, body wall muscle, distal tip cell, posterior intestine, and hypodermal seam cells. Adult hermaphrodites are shown. Scale bars represent 10 μm (A), 5 μm (B-E). (F) GFP tagged PPK-1 expressed in neurons under the *rab-3* promoter. Scale bar represents 5 μm. (G) A single section of the nerve ring at increased magnification shows localization of GFP at cell body plasma membrane. Scale bar represents 5 μm. L2 larva is shown.

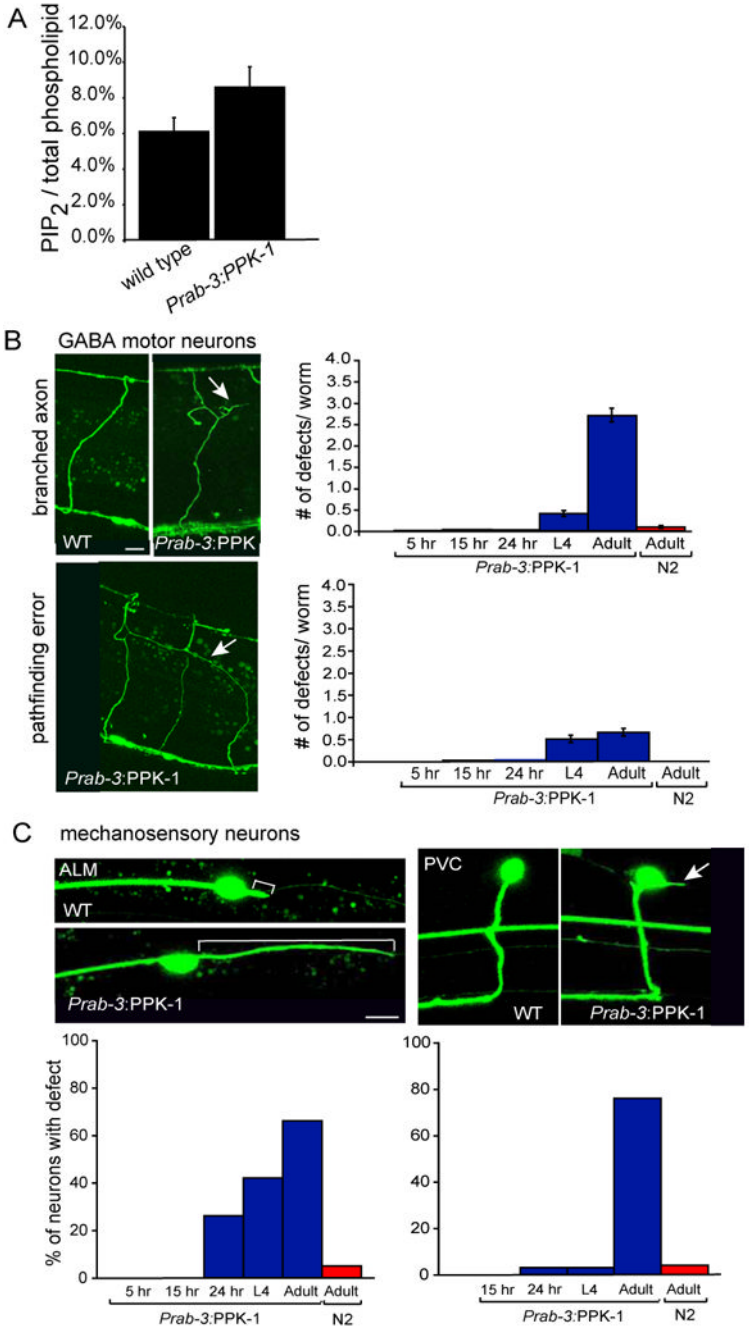


**Figure 3.**

Overexpression of PPK-1 under the pan-neuronal promoter *rab-3* causes an accumulation of $PIP_2$ and neuronal defects.

(A) Graph of $PIP_2$ levels as a percentage of total labeled phospholipids in wild type and *Prab-3*::PPK-1 animals. An average of three biological replicates for each genotype is shown, p=0.018 unpaired-T test. (B) Accumulation of branched axons and pathfinding errors are observed starting in L4 larvae. Marker: *Punc-47*:GFP (GABA:GFP). Scale bar represents 10 μm. Percent of worms showing abnormally branched axon and/or pathfinding errors: 5 hours-1%, 15 hours-4%, 24 hours-7%, L4-54%, one day adult-90%. Worms also have an

increased number of commissures that migrate on the wrong side (not shown). (C) Accumulation of extended posterior projections from ALM cell bodies, and projections from the PVC cell body are also observed late after development. Marker: *Pmec-7:*GFP. Because single neurons were analyzed, the % of neurons affected is shown. Scale bar represents 5 μm.

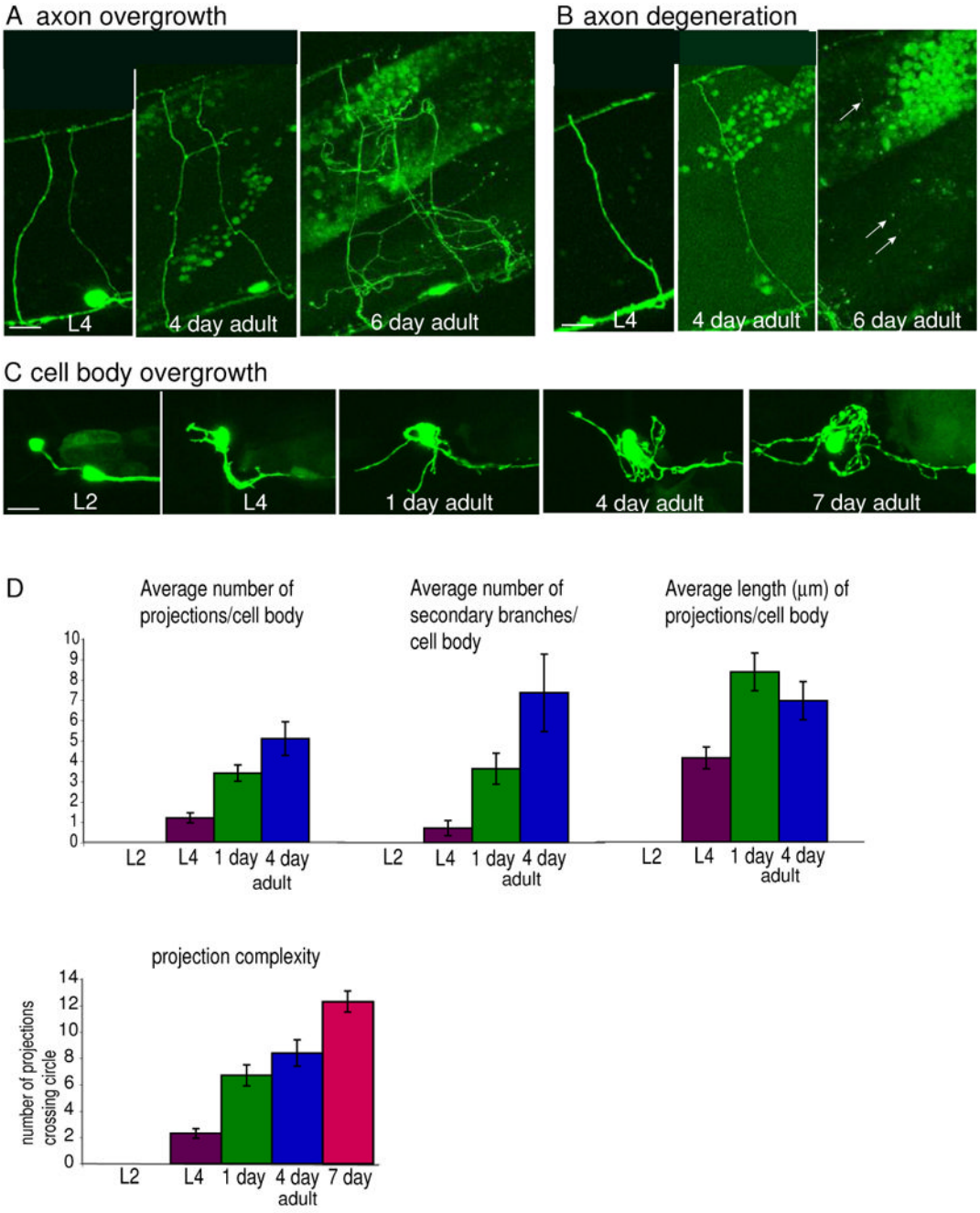


**Figure 4.**

Longitudinal study showing progressive defects in adult *Prab-3*:PPK-1 animals.

(A) Example of axon overgrowth. A single region in the middle of the body of a worm imaged as an L4, 4 day old adult, and six day old adult is shown. Lateral view. (B) Example of axon degeneration. A single region in the middle of the body of a worm imaged as an L4, 4 day old adult, and six day old adult. Lateral view. (C) Example of cell body overgrowth. The DVB neuron in the tail of a worm was imaged when the animal was an L2, L4, 1 day, 4 day, and 7 day old adult. Lateral view is shown. (D) Quantification of progressive cell body overgrowth. Images were analyzed for specific defects: the number of projections extending from the cell body, number of secondary branched projections, and length of the longest projection. For the

length measurement, if one projection had multiple branches, then only the longest branch was measured starting from the point of contact with the cell body. Only images collected between L4 and four day old adults were analyzed. Seven day old neurons could not be quantified using this method due to extensive branching, overlapping processes, and degenerating processes. Significant increases in all categories are seen from L4 stage to first day adult. Neuron complexity was quantified by drawing 5μm, 6 μm, 7 μm, and 8 μm diameter circles around the DVB neuron cell body placing the cell body in the center of the circle. The number of times a projection crossed the circle was determined for each circle, and the four numbers were averaged for each time point (unless the projections were shorter than a circle, in which case the average was taken of the smaller circles). No significant difference was found for the number of projections crossing different sized circles for a given cell body at a given time point, suggesting that complexity near the base is similar to complexity further away from the cell body. Each bar in the graph shows an average for the five worms that survived to seven day old adults. Scale bars represent 5 μm.

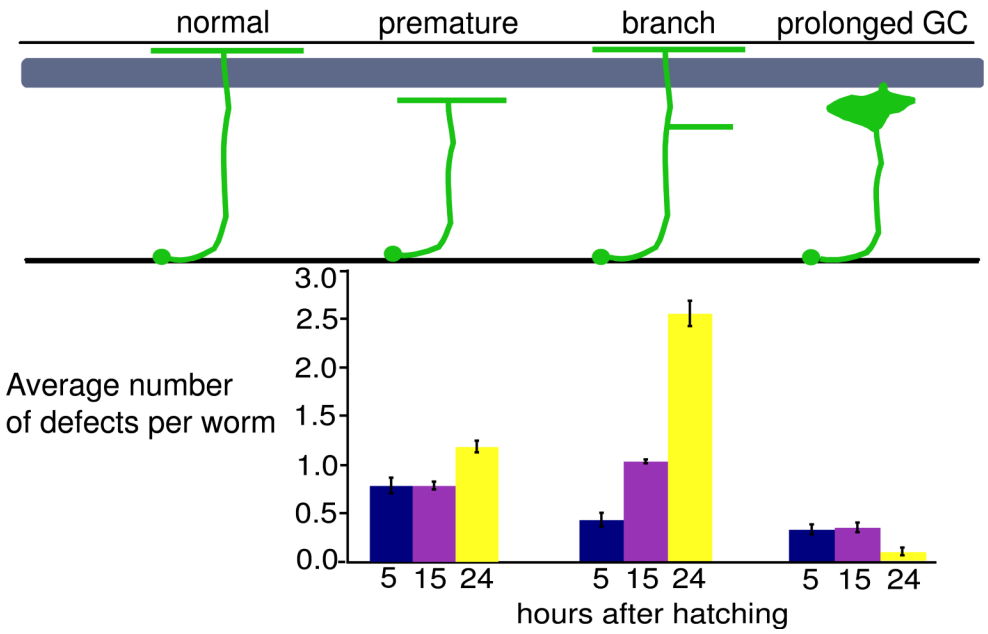


**Figure 5.**

Quantitative analysis of defects in animals overexpressing PPK-1 in developing GABA neurons. Synchronized egg lay collections were taken and animals were aged and defects were scored 5, 15, and 24 hours after hatching at 25°C. The timing should approximate L1, L2, and L3 larval stages. Percent of animals with specific defects: premature axon termination, 5 hr- 55%, 15hr- 51%, 24 hr- 42%; branched axons, 5 hr- 35%, 15 hr- 74%, 24 hr- 96%; prolonged growth cone, 5 hr- 28%, 15 hr- 26%, 24 hr-10%. Many worms at all stages had multiple defects. Worms also have an increased number of commissures that migrate on the wrong side (not shown). No significant defects in any category were observed in wild type animals. Grey box represents the body wall muscle.

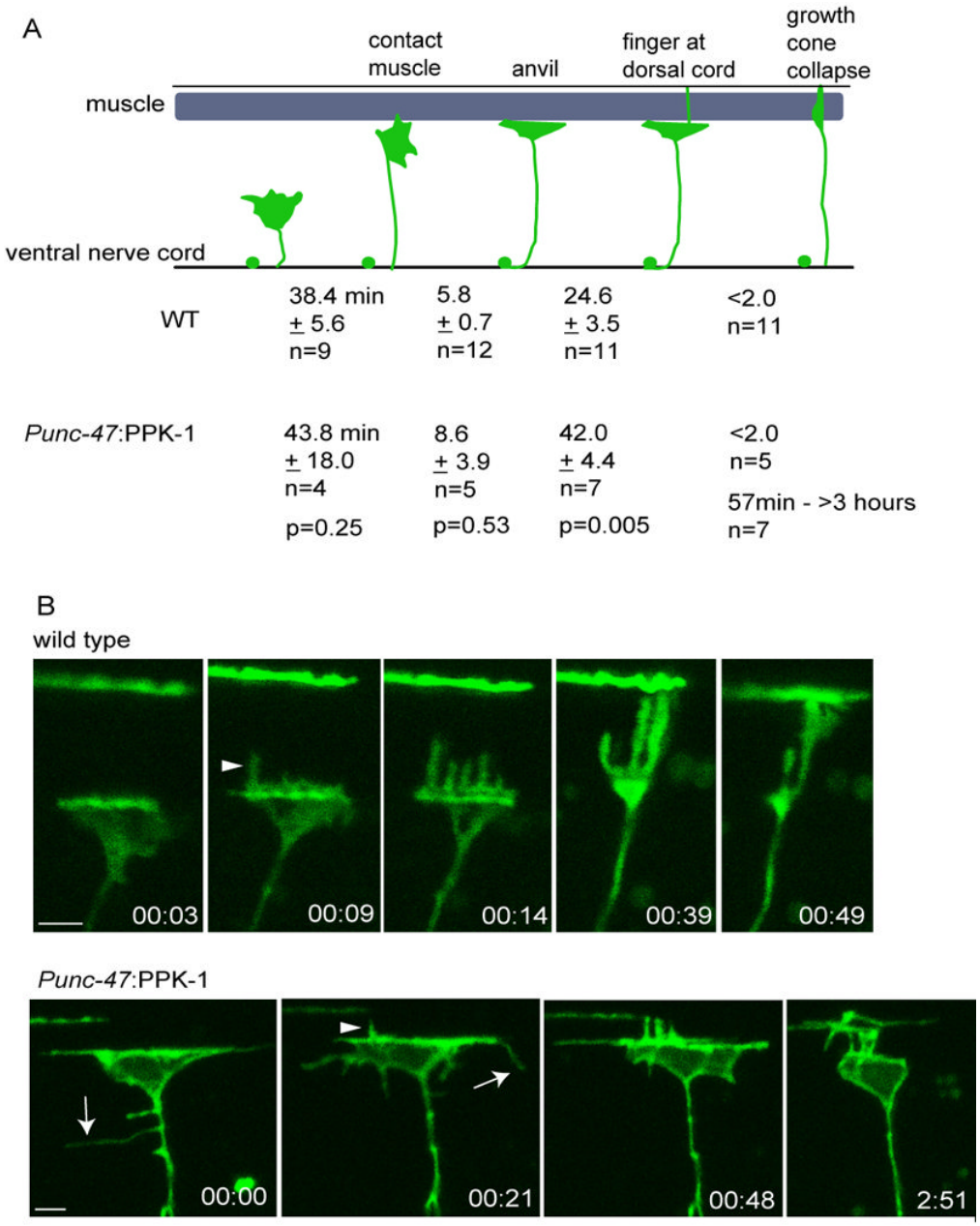


**Figure 6.**

Time-lapse imaging of growth cones in wild type and animals overexpressing PPK-1.

(A) Average time wild type and *Punc-47*:PPK-1 growth cones take to reach the dorsal muscle, form an anvil, send a projection to the dorsal cord, and collapse.

(B) Example images of wild type and *Punc-47*::PPK-1 growth cones taken from supplemental movies 2 and 3 respectively. Wild type growth cone forms an anvil, extends fingers and collapses. Time in hours and minutes is shown. *Punc-47*:PPK-1 growth cone is also shown at the muscle boundary as imaging began. Fingers extend to the dorsal cord and the growth cone begins to collapse, but fails to fully collapse after 2 hours and 51 minutes. Ectopic projections are marked by arrows and dorsal projections by arrow heads.

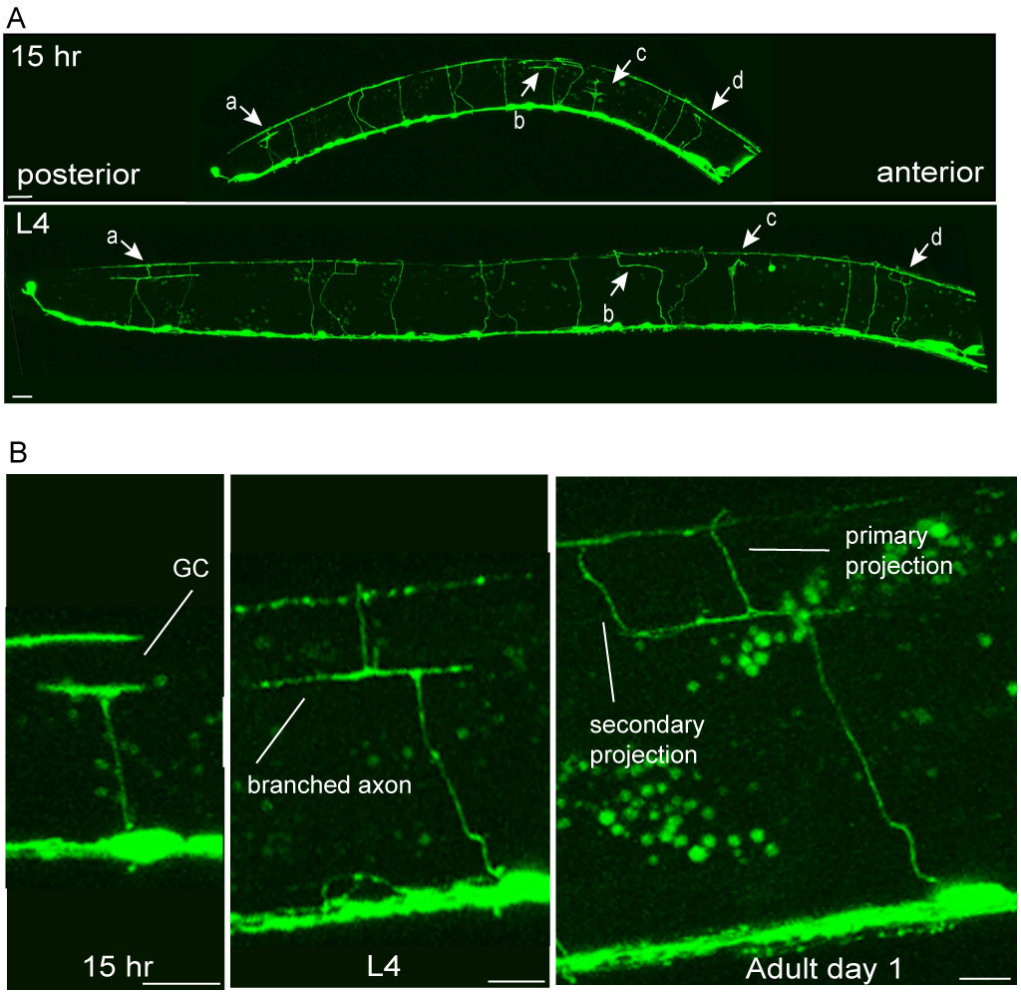


**Figure 7.**

Longitudinal study showing how abnormal structures resolve as development proceeds. (A) Entire worm 15 hours after hatching (L2) and L4 larval stages. Prolonged growth cones: a, b, c, d are marked by arrows. All four send projections to the dorsal cord by the L4 larval stage (for c, a very thin projection is visible). Scale bars represent 10 μm. (B) High magnification of a prolonged growth cone from a different worm. Section of the worm showing a prolonged growth cone (approximately 15 hours after hatching) which resolves into an axon that branches at the dorsal muscle (L4), and finally forms a secondary projection (1 day adult). Scale bars represent 5 μm.